Article

Theoretical Study of C–H and N–H σ-Bond Activation Reactions by Titinium(IV)-Imido Complex. Good Understanding Based on Orbital Interaction and Theoretical Proposal for N–H σ-Bond Activation of Ammonia

Noriaki Ochi, Yoshihide Nakao, Hirofumi Sato, and Shigeyoshi Sakaki

J. Am. Chem. Soc., **2007**, 129 (27), 8615-8624• DOI: 10.1021/ja071825c • Publication Date (Web): 19 June 2007

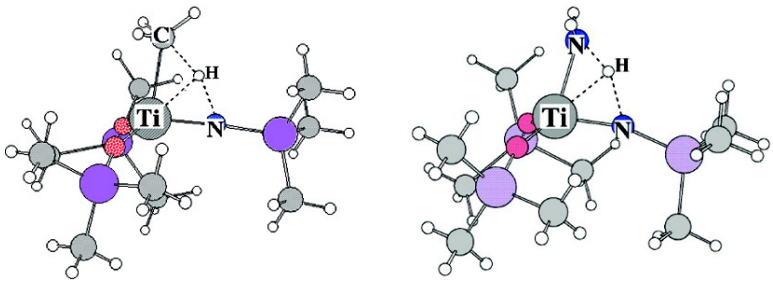

C-H activation of CH_4 **N-H activation of NH_3**

More About This Article

Additional resources and features associated with this article are available within the HTML version:

- Supporting Information
- Access to high resolution figures
- Links to articles and content related to this article
- Copyright permission to reproduce figures and/or text from this article

View the Full Text HTML

J|A|C|S
ARTICLES
Published on Web 06/19/2007

Theoretical Study of C−H and N−H σ-Bond Activation Reactions by Titinium(IV)-Imido Complex. Good Understanding Based on Orbital Interaction and Theoretical Proposal for N−H σ-Bond Activation of Ammonia

Noriaki Ochi,[†] Yoshihide Nakao,[†] Hirofumi Sato,[†] and Shigeyoshi Sakaki*[,†,‡]

Contribution from the Department of Molecular Engineering, Graduate School of Engineering, Kyoto University, Nishikyo-ku, Kyoto 615-8510, Japan, and Fukui Institute for Fundamental Chemistry, Nishihiraki-cho, Takano, Sakyo-ku 610-8103, Japan

Received March 15, 2007; E-mail: sakaki@moleng.kyoto-u.ac.jp

Abstract: The C−H σ-bond activation of methane and the N−H σ-bond activation of ammonia by $(Me_3SiO)_2Ti(=NSiMe_3)$ **1** were theoretically investigated with DFT, MP2 to MP4(SDQ), and CCSD(T) methods. The C−H σ-bond activation of methane takes place with an activation barrier (E_a) of 14.6 (21.5) kcal/mol and a reaction energy (ΔE) of −22.7 (−16.5) kcal/mol to afford $(Me_3SiO)_2Ti(Me)\{NH(SiMe_3)\}$, where DFT- and MP4(SDQ)-calculated values are given without and in parentheses, respectively, hereafter. The electron population of the CH_3 group increases, but the H atomic population decreases upon going to the transition state from the precursor complex, which indicates that the C−H σ-bond activation occurs in heterolytic manner unlike the oxidative addition. The Ti atomic population considerably increases upon going to the transition state from the precursor complex, which indicates that the charge transfer (CT) occurs from methane to Ti. These population changes are induced by the orbital interactions among the $d_\pi-p_\pi$ bonding orbital of the $Ti{=}NSiMe_3$ moiety, the Ti d_{z^2} orbital and the C−H σ-bonding and σ^*-antibonding orbitals of methane. The reverse regioselective C−H σ-bond activation which leads to formation of $(Me_3SiO)_2Ti(H)\{NMe(SiMe_3)\}$ takes place with a larger E_a value and smaller exothermicity. The reasons are discussed in terms of Ti−H, Ti−CH_3, Ti−NH_3, N−H, and N−CH_3 bond energies and orbital interactions in the transition state. The N−H σ-bond activation of ammonia takes place in a heterolytic manner with a larger E_a value of 19.0 (27.9) kcal/mol and considerably larger exothermicity of −45.0 (−39.4) kcal/mol than those of the C−H σ-bond activation. The N−H σ-bond activation of ammonia by a Ti-alkylidyne complex, $[(PNP)Ti(\equiv CSiMe_3)]$ **3** (PNP = N-[2-$(PH_2)_2$-phenyl]$_2^-$]) ,was also investigated. This reaction takes place with a smaller E_a value of 7.5 (15.3) kcal/mol and larger exothermicity of −60.2 (−56.1) kcal/mol. These results lead us to predict that the N−H σ-bond activation of ammonia can be achieved by these complexes.

Introduction

C−H σ-bond activation of alkane by a transition metal complex is one of the most challenging reactions in organometallic chemistry, inorganic chemistry, and catalytic chemistry, because a functional group can be introduced into alkane via C−H σ-bond activation.[1] In the recent review articles,[1] we found three categories of σ-bond activation, as follows; (1) C−H σ-bond activation via oxidative addition reaction by late transition metal complexes, (2) C−H σ-bond activation via σ-bond metathesis by lanthanide and actinide complexes, and (3) C−H σ-bond activation via addition of the C−H σ-bond across M=N and M=C multiple bonds by early to middle transition metal complexes.

The oxidative addition of a C−H σ-bond to late transition metal complexes such as platinum(0) and platinum(II) complexes has been theoretically investigated by many groups.[2−15] From those theoretical studies, we have now detailed knowledge

[†] Kyoto University.
[‡] Fukui Institute for Fundamental Chemistry.

(1) Recent reviews: (a) Arndtsen, B. A.; Bergman, R. G.; Mobley, T. A.; Peterson, T. H. *Acc. Chem. Res.* **1995**, *28*, 154. (b) Shilov, A. E.; Shul'pin, G. B. *Chem. Rev.* **1997**, *97*, 2879. (c) Jones, W. D. *Top. Organomet. Chem.* **1999**, *3*, 9. (d) Sen, A. *Top. Organomet. Chem.* **1999**, *3*, 81. (e) Crabtree, R. H. *J. Chem. Soc., Dalton Trans.* **2001**, 2437. (f) Labingerand, J. A.; Bercaw, J. E. *Nature* **2002**, *417*, 507.
(2) Saillard, J. -Y.; Hoffmann. R. *J. Am. Chem. Soc.* **1984**, *106*, 2006.
(3) (a) Obara, S.; Kitaura, K.; Morokuma, K. *J. Am. Chem. Soc.* **1984**, *106*, 7482. (b) Koga, N.; Morokuma, K. *J. Phys. Chem.* **1990**, *94*, 5454. (c) Koga, N.; Morokuma, K. *J. Am. Chem. Soc.* **1993**, *115*, 6883. (d) Matsubara, T.; Koga, N.; Musaev, D. G.; Morokuma, K. *J. Am. Chem. Soc.* **1998**, *120*, 12692.
(4) (a) Low, J. J.; Goddard, W. A., III. *J. Am. Chem. Soc.* **1986**, *108*, 6115. (b) Low, J. J.; Goddard, W. A., III. *Organometallics* **1986**, *5*, 609.
(5) (a) Blomberg, M. R. A.; Siegbahn, P. E. M.; Nagashima, U.; Wennerberg, J. *J. Am. Chem. Soc.* **1991**, *113*, 424. (b) Svensson, M.; Blomberg, M. R. A.; Siegbahn, P. E. M. *J. Am. Chem. Soc.* **1991**, *113*, 7076. (c) Blomberg, M. R. A.; Siegbahn, P. E. M.; Svensson, M. *J. Am. Chem. Soc.* **1992**, *114*, 6095. (d) Siegbahn, P. E. M.; Blomberg, M. R. A.; Svensson, M. *J. Am. Chem. Soc.* **1993**, *115*, 4191. (e) Blomberg, M. R. A.; Siegbahn, P. E. M.; Svensson, M. *J. Phys. Chem.* **1994**, *98*, 2062. (f) Siegbahn, P. E. M.; Blomberg, M. R. A. *Organometallics* **1994**, *13*, 354. (g) Siegbahn, P. E. M. *Organometallics* **1994**, *13*, 2833. (h) Siegbahn, P. E. M.; Svensson, M. *J. Am. Chem. Soc.* **1994**, *116*, 10124. (i) Siegbahn, P. E. M. *J. Am. Chem. Soc.* **1996**, *118*, 1487. (j) Siegbahn, P. E. M.; Crabtree, R. H. *J. Am. Chem. Soc.* **1996**, *118*, 4442.
(6) (a) Song, J.; Hall, M. B. *Organometallics* **1993**, *12*, 3118. (b) Jimenez-Catano, R.; Hall, M. B. *Organometallics* **1996**, *15*, 1889. (c) Niu, S.-Q.; Hall, M. B. *J. Am. Chem. Soc.* **1998**, *120*, 6169.

about the oxidative addition reaction. The C−H σ-bond addition across the M═N bond in the early transition metal complexes has been theoretically investigated by Cundari and his collaborators in the past decade.[16] They also investigated an interesting bonding nature of the transition metal imido complexes, transition metal alkylidene complexes, and their methane adducts.[17] Recently, the C−H σ-bond activation of benzene by the Ti-alkylidyne complex was also experimentally succeeded and theoretically investigated with the DFT method.[18] However, many issues to be investigated still remain; for instance, comparison of the C−H σ-bond activation between early and late transition metal complexes has not been made yet, to our knowledge, despite that such a comparison is of considerable interest. Also, it is not clear what orbital interaction plays an important role in the C−H σ-bond activation by the M═N bond.

N−H σ-bond activation of ammonia by transition metal complexes is another challenging research target. Though one successful result has been reported recently,[19] the N−H σ-bond activation of ammonia is still difficult. Ammonia can form stable complexes with late transition metal elements, while early transition metal complexes of ammonia are less known than the late transition metal complexes. Because the formation of a too stable reactant complex of ammonia is one of the important reasons for difficulty in the N−H σ-bond activation of ammonia,[19] it is of considerable interest to investigate whether or not early transition-metal complexes can be utilized for the N−H σ-bond activation of ammonia.

In this theoretical work, we investigated the C−H σ-bond activation of methane and the N−H σ-bond activation of ammonia with a Ti-imido complex by DFT, MP2 to MP4(SDQ), and CCSD(T) methods. Our purposes here are to show the differences in the C−H σ-bond activation between early and late transition metal complexes, to clarify what orbital interaction plays an important role in the C−H σ-bond activation by this complex, and to present a theoretical prediction of whether or not the Ti-imido complex can be applied to the N−H σ-bond activation of ammonia. The N−H σ-bond activation by Ti-alkylidyne complex was also theoretically investigated, because the C−H σ-bond activation of benzene was achived by the Ti-alkylidyne complex.[18]

Computational Details

Geometries were optimized with the DFT method, where the B3LYP functional was used for exchange-correlation terms.[20−22] We ascertained that each equilibrium geometry exhibited no imaginary frequency and each transition state exhibited one imaginary frequency. We carried out IRC calculations, to check that the transition state connected the reactant and product. Energy and population changes were evaluated with the DFT(B3LYP), MP2 to MP4(SDQ), and CCSD(T) methods, using the DFT-optimized geometries. In MP2 to MP4(SDQ) and CCSD(T) calculations, core orbitals were excluded from active space. Two kinds of basis set systems were used. The smaller system (BS1) was used for geometry optimization. In this BS1, core electrons of Ti (up to 2p) and Pt (up to 4f) were replaced with effective core potentials (ECPs),[23] and their valence electrons were represented with (541/541/311) and (541/541/111) basis sets,[23,24] respectively. For Si and P, core electrons (up to 2p) were replaced with ECPs,[25] and their valence electrons were represented with (21/21/1) basis sets,[25] where a d-polarization function was added.[26] For H, C, N, and O, 6-31G* basis sets[27] were employed, where a p-polarization function was added for the active H atom that reacts with Ti complexes to form either C−H or N−H bond, and a diffuse function was added to the N atom. The better basis set system (BS2) was used for evaluation of energy changes. In the BS2 system, (5311/5311/311/1) and (5311/5311/111/1) basis sets[23,24,28] were employed for Ti and Pt, respectively, where the same ECPs as those of BS1 were employed for core electrons. For H, C, N, O, Si, and P, the 6-311G* basis sets were employed,[29−31] where a p-polarization function was added to the active H atom and a diffuse function was added to the imido N and alkylidyne C atoms. Zero-point energy was evaluated with the DFT/BS1 method, under the assumption of a harmonic oscillator.

The Gaussian 03 program package[32] was used for all calculations. Population analysis was carried out with the method of Weinhold et al.[33] Molecular orbitals were drawn with the MOLEKEL program package.[34]

(7) (a) Sakaki, S.; Ieki, M. *J. Am. Chem. Soc.* **1993**, *115*, 2373. (b) Sakaki, S.; Biswas, B.; Sugimoto, M. *J. Chem. Soc., Dalton Trans.* **1997**, 803. (c) Sakaki, S.; Biswas, B.; Sugimoto, M. *Organometallics* **1998**, *17*, 1278. (d) Sakaki, S.; Mizoe, M.; Musashi, Y.; Biswas, B.; Sugimoto, M. *J. Phys. Chem. A* **1998**, *102*, 8027. (e) Biswas, B.; Sugimoto, M.; Sakaki, S. *Organometallics* **2000**, *19*, 3895. (f) Sakaki, S. *Top. Organomet. Chem.* **2005**, *12*, 31.
(8) Hinderling, C.; Feichtinger, D.; Plattner, D. A.; Chen, P. *J. Am. Chem. Soc.* **1997**, *119*, 10793.
(9) Su, M.-D.; Chu, S.-Y. *J. Am. Chem. Soc.* **1997**, *119*, 5373.
(10) Espinosa-Garcia, J.; Corchado, J. C.; Truhlar, D. G. *J. Am. Chem. Soc.* **1997**, *119*, 9891.
(11) Hill, G. S.; Puddephatt, R. J. *Organometallics* **1998**, *17*, 1478.
(12) (a) Heiberg, H.; Swang, O.; Ryan, O. B.; Gropen, O. *J. Phys. Chem. A* **1999**, *103*, 10004. (b) Heiberg, H.; Johansson, L.; Gropen, O.; Ryan, O. B.; Swang, O.; Tilset, M. *J. Am. Chem. Soc.* **2000**, *122*, 10831.
(13) Ustynyuk, Y. A.; Ustynyuk, L. Y.; Laikov, D. N.; Lunin, V. V. *J. Organomet. Chem.* **2000**, *597*, 182.
(14) Bartlett, K. L.; Goldberg, K. I.; Borden, W. T. *Organometallics* **2001**, *20*, 2669.
(15) (a) Kua, J.; Xu, X.; Periana, R. A.; Goddard, W. A., III. *Organometallics* **2002**, *21*, 511. (b) Xu, X.; Kua, J.; Periana, R. A.; Goddard, W. A., III. *Organometallics* **2003**, *22*, 2057.
(16) (a) Cundari, T. R. *J. Am. Chem. Soc.* **1992**, *114*, 10557. (b) Cundari, T. R. *Organometallics* **1993**, *12*, 1998. (c) Cundari, T. R. *Organometallics* **1993**, *12*, 4971. (d) Cundari, T. R. *J. Am. Chem. Soc.* **1994**, *116*, 340. (e) Benson, M. T.; Cundari, T. R.; Moody, E. W. *J. Organomet. Chem.* **1995**, *504*, 1. (f) Cundari, T. R.; Matsunaga, N.; Moody, E. W. *J. Phys. Chem.* **1996**, *100*, 6475. (g) Cundari, T. R.; Klinchkman, T. R.; Wolczanski, P. T. *J. Am. Chem. Soc.* **2002**, *124*, 1481.
(17) (a) Cundari, T. R. *Chem. Rev.* **2000**, *100*, 807. (b) Cundari, T. R.; Gordon, M. S. *J. Am. Chem. Soc.* **1991**, *113*, 5231. (c) Cundari, T. R.; Gordon, M. S. *J. Am. Chem. Soc.* **1992**, *114*, 539. (d) Cundari, T. R. *J. Am. Chem. Soc.* **1992**, *114*, 7879. (e) Cundari, T. R. *J. Am. Chem. Soc.* **1992**, *114*, 10557. (f) Cundari, T. R. *Organometallics* **1993**, *12*, 1998.
(18) Bailey, B. C.; Fan, H.; Baum, E. W.; Huffman, J. C.; Baik, M.-H.; Mindiola, D. J. *J. Am. Chem. Soc.* **2005**, *127*, 16016.
(19) (a) Zhao, J.; Goldman, A. S.; Hartwig, J. F. *Science* **2005**, *307*, 1080. (b) Kanzelberger, M.; Zhang, X.; Emge, T. J.; Goldman, A. S.; Zhao, J.; Incarvito, C.; Hartwig, J. F. *J. Am. Chem. Soc.* **2003**, *125*, 13644.
(20) Becke, A. D. *Phys. Rev.* **1988**, *A38*, 3098.
(21) Becke, A. D. *J. Chem. Phys.* **1983**, *98*, 5648.
(22) Lee, C.; Yang, W.; Parr, R. G. *Phys. Rev.* **1988**, *B37*, 785.
(23) Hay, P. J.; Wadt, W. R. *J. Chem. Phys.* **1985**, *82*, 299.
(24) Couty, M.; Hall, M. B. *J. Comput. Chem.* **1996**, *17*, 1359.
(25) Wadt, W. R.; Hay, P. J. *J. Chem. Phys.* **1985**, *82*, 284.
(26) Höllowarth, A.; Böhme, M.; Dapprich, S.; Ehlers, A. W.; Gobbi, A.; Jonas, V.; Köhler, K. F.; Stegmann, R.; Veldkamp, A.; Frenking, G. *Chem. Phys. Lett.* **1993**, *208*, 237.
(27) (a) Hariharan, P. C.; Pople, J. A. *Theor. Chim. Acta* **1973**, *28*, 213. (b) Hariharan, P. C.; Pople, J. A. *Mol. Phys.* **1974**, *27*, 209.
(28) Ehlers, A. W.; Böhme, M.; Dapprich, S.; Gobbi, A.; Höllwarth, A.; Jonas, V.; Köhler, K. F.; Stegmann, R.; Veldkamp, A.; Frenking, G. *Chem. Phys. Lett.* **1993**, *208*, 111.
(29) Krishnan, R.; Binkley, J. S.; Seeger, R.; Pople, J. A. *J. Chem. Phys.* **1980**, *72*, 650.
(30) McLean, A. D.; Chandler, G. S. *J. Chem. Phys.* **1980**, *72*, 5639.
(31) Blaudeau, J.-P.; McGrath, M. P.; Curtiss, L. A.; Radom, L. *J. Chem. Phys.* **1997**, *107*, 5016.
(32) Pople, J. A., et al. *Gaussina 03*, revision C.02; Gaussian, Inc.: Wallingford, CT, 2004.
(33) Reed, A. E.; Curtiss, L. A.; Weinhold, F. *Chem. Rev.* **1988**, *88*, 899.
(34) Flükiger, P.; Lüthi, H. P.; Portann, S.; Weber, J. *MOLEKEL*, v.4.3; Scientific Computing: Manno, Switzerland, 2002−2002. Portman, S.; Lüthi, H. P. *CHIMIA* **2000**, *54*, 766.

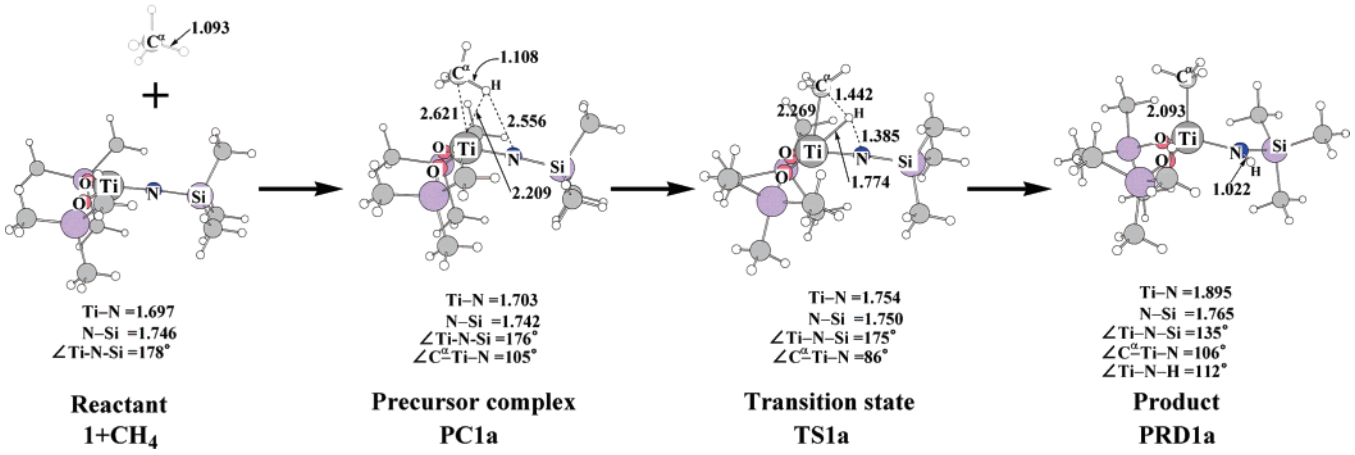

Figure 1. Geometry changes in the C—H σ-bond activation of methane by $(Me_3SiO)_2Ti(=NSiMe_3)$ **1**. Bond lengths are in angstroms, and bond angles are in degrees.

Results and Discussion

Geometry and Energy Changes by the C—H σ-Bond Activation of Methane by Ti-Imido Complex, $[(Me_3SiO)_2Ti(=NSiMe_3)]$ 1. The C—H σ-bond activation of methane by a Ti-imido complex, $[(Me_3SiO)_2Ti(=NSiMe_3)]$ **1**, takes place through a precursor complex (**PC1a**) and transition state (**TS1a**), to afford a product complex (**PRD1a**), as shown in Figure 1.

In $[(Me_3SiO)_2Ti(=NSiMe_3)]$ **1**, the Ti—N—Si moiety is almost linear (175°), which agrees well with the experimental value (175°) of a similar complex.[35] This linear geometry of the $Ti=NSiMe_3$ group indicates that the $NSiMe_3$ moiety is considered to be an anion, as reported.[17a,d] The optimized Ti—N bond (1.697 Å) is moderately shorter and the optimized N—Si bond (1.746 Å) is moderately longer than those of the similar complex,[36] though the differences are not large. We optimized the model complex with several functionals and a variety of basis sets but found moderately longer Ti—N and moderately shorter N—Si distances in all the optimized geometries (see Supporting Information Figure S1 and Tables S1 and S2). In **PC1a**, methane approaches the Ti center, where the Ti—C^α and Ti—H distances are 2.621 Å and 2.209 Å, respectively, where C^α represents the C atom of methane, hereafter. The C^α—H bond slightly lengthens to 1.108 Å, which is similar to that of the agostic interaction system. Because the d orbital is not occupied in the Ti(IV) center in a formal sense, the charge transfer (CT) from the C—H bonding orbital to the empty d orbital of Ti is considered to be the origin of the bonding interaction. This is essentially the same as the agostic interaction.[37–39] In **TS1a**, the Ti—C^α distance shortens to 2.269 Å which is similar to that of **PRD1a**. The C^α—H distance considerably lengthens to 1.442 Å, whereas the N—H distance (1.385 Å) is still long. The H atom that is moving from the C^α atom to the N atom is at the middle position between C^α and N atoms. The similar geometry changes were reported in the theoretical study of the heterolytic C—H σ-bond activation of methane by $Pd(\eta^2\text{-}O_2CH)_2$ and $Pt(\eta^2\text{-}O_2CH)_2$.[7e] The product **PRD1a** takes a pseudo-tetrahedral structure, as expected from the d^0 electron configuration.

Table 1. Binding Energy (BE), Activation Barrier (E_a), and Reaction Energy (ΔE) of the C—H σ-Bond Activation of Methane by $(Me_3SiO)_2Ti(=NSiMe_3)$ **1** and $(H_3SiO)_2Ti(=NSiH_3)$ **1m**[a]

	$(Me_3SiO)_2Ti(=NSiH_3)$ + CH_4			$(H_3SiO)_2Ti(=NSiH_3)$ + CH_4		
	BE[b]	E_a[c]	ΔE[d]	BE[b]	E_a[c]	ΔE[d]
MP2	−9.8	17.6	−16.5	−9.6	18.7	−14.9
MP3	−7.1	12.7	−36.5	−7.0	12.9	−35.4
MP4(DQ)	−7.8	18.0	−25.3	−7.8	18.7	−24.2
MP4(SDQ)	−9.4	21.5	−16.5	−9.4	22.8	−14.6
CCSD(T)	-	-	-	−9.0	17.0	−22.7
DFT(B3LYP)	−4.5	14.6	−22.7	−5.5	15.5	−22.6

[a] In kcal/mol unit. [b] BE = E_t(precursor complex) − E_t(sum of reactants). [c] E_a = E_t(transition state) − E_t(precursor complex). [d] ΔE = E_t(product) − E_t(sum of reactants).

Binding energy (BE), activation barrier (E_a), and reaction energy (ΔE) are defined as the energy differences between **PC1a** and the sum of reactants, between **PC1a** and **TS1a**, and between **PRD1a** and the sum of reactants, respectively. A negative ΔE value means that the C—H σ-bond activation is exothermic and vice versa. First, we calculated BE, E_a, and ΔE values in the reaction of a model Ti-imido complex, $[(H_3SiO)_2Ti(=NSiH_3)]$ **1m**, in which the methyl groups are replaced by the H atoms, because **1** is too large to perform CCSD(T) calculations; geometry changes of this model reaction are given in Supporting Information Figure S2. In the reaction of **1m**, the BE value fluctuates little upon going to CCSD(T) from MP2, as shown in Table 1, while the DFT-calculated BE value is somewhat smaller than the others.[40] These results indicate that the BE values calculated by the DFT and MP4(SDQ) methods are reliable. The E_a and ΔE values somewhat fluctuate around MP2 and MP3 levels but much less upon going to CCSD(T) from MP3. The DFT- and MP4(SDQ)-calculated BE, E_a, and ΔE values show little difference between **1** and **1m**, suggesting that the model system is useful to investigate this type of C—H σ-bond activation. It is noted that the DFT-calculated E_a and ΔE values are similar to those of the CCSD(T)-calculated values, while the MP4(SDQ)-calculated E_a value is considerably larger

(35) (a) Haymore, B. L.; Maatta, E. A.; Wentworth, R. D. *J. Am. Chem. Soc.* **1979**, *101*, 2063. (b) Parkin, G.; van Asselt, A.; Leahy, D. J.; Whinnery, L.; Hua, N. G.; Quan, R. W.; Henling, L. M.; Schaefer, W. P.; Santarsiero, B. D.; Bercaw, J. E. *Inorg. Chem.* **1992**, *31*, 82.
(36) Bennett, J. L.; Wolczanski, P. T. *J. Am. Chem. Soc.* **1997**, *119*, 10696.
(37) Koga, N.; Obara, S. Morokuma, K. *J. Am. Chem. Soc.* **1984**, *106*, 4625.
(38) Goddard, R. J.; Hoffmann, R.; Jemmis, E. D. *J. Am. Chem. Soc.* **1980**, *102*, 7667.
(39) Obara, S.; Koga, N.; Morokuma, K. *J. Organomet. Chem.* **1984**, *270*, C33.
(40) (a) The interaction energy between π-conjugated systems and $Pt(PH_3)_2$ is also underestimated by the DFT method, similarly.[40b] (b) Kameno, Y.; Ikeda, A.; Nakao, Y.; Sato, H.; Sakaki, S. *J. Phys. Chem.* **2005**, *109*, 8055.

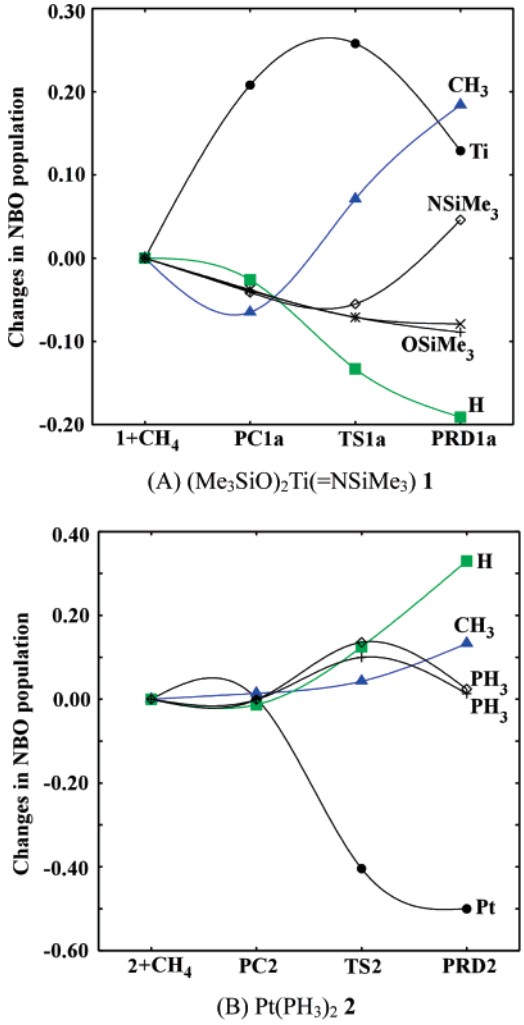

Figure 2. Population changes in C−H σ-bond activations of methane by (A) $(Me_3SiO)_2Ti(=NSiMe_3)$ **1** and (B) $Pt(PH_3)_2$ **2**. The positive value represents the increase in electron population, and vice versa. The B3LYP/BS2 method was employed.

and the MP4(SDQ)-calculated exothermicity is considerably smaller than the CCSD(T)-calculated values.[41]

Though the DFT method underestimates the BE value, we employed the DFT method to discuss the E_a and ΔE values of the reaction of **1**, because our main purpose is to investigate how much easily the C−H σ-bond activation takes place; note that **1** + CH_4 is too large to perform CCSD(T) calculation.

Important Orbital Interactions in the C−H σ-Bond Activation by Ti-Imido Complex. It is of considerable importance to clarify the characteristic features of the C−H σ-bond activation of methane by the Ti-imido complex. We compared the C−H σ-bond activation reaction with the oxidative addition of methane to $Pt(PH_3)_2$ **2**, because the latter reaction is one of the most typical C−H σ-bond activations through the oxidative addition. We optimized the precursor complex, the transition state, and the product of this oxidative addition, using the DFT/BS1 method. The explanation of geometry and energy changes are omitted here because this reaction was theoretically investigated previously,[4,7a,d] and no essential difference from the previous works was observed; see Supporting Information Figure S3 for the geometry changes.

(41) Usually, the energy changes are less converged in the MP4 calculations than in the DFT calculations upon going from poor basis sets to good ones. Also, the energy changes tend not to converge upon going from MP2 to MP4, when the quality of the Hartree−Fock wavefunction is not good. On the other hand, the DFT method tends to underestimate the interaction energy between the transition metal and coordinating substrate.[40] Thus, we must carefully check if the energy changes calculated by the MP2 to MP4 and DFT methods are considerably different or not. It is noted however that a considerable difference is not observed when the electron correlation effect is not large and the sufficiently good basis sets are used.

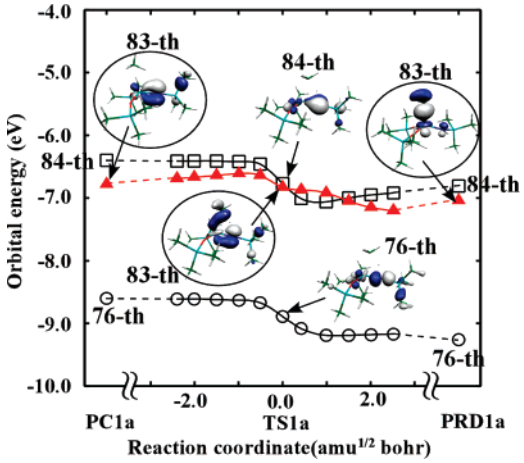

Figure 3. Orbital energy changes in C, IIIH σ-bond activations of methane by $(Me_3SiO)_2Ti(=NSiMe_3)$ **1**.

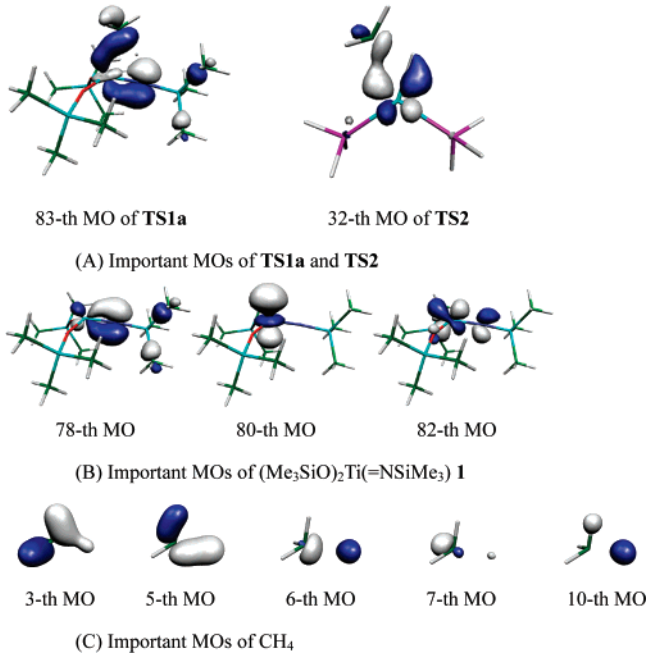

Figure 4. Important MOs in **TS1a** and **TS2**, and fragment MOs of $(Me_3SiO)_2Ti(=NSiMe_3)$ **1** and methane. The B3LYP/BS2 method was employed.

Electron population changes are compared between the C−H σ-bond activation reactions by **1** and **2**, as shown in Figure 2. In the oxidative addition of methane to **2**, the electron populations of H and CH_3 groups increase but the Pt atomic population considerably decreases, as the reaction proceeds (Figure 2B). These population changes are consistent with our understanding that this is the oxidative addition. Population changes in the C−H σ-bond activation by **1** are significantly different from those in the reaction by **2**, as follows: (1) The electron population of CH_3 increases very much, as shown in Figure 2A. (2) The H atomic population considerably decreases upon going from **PC1a** to **PRD1a** in the reaction of **1**. (3) The Ti atomic population considerably increases upon going to **TS1a**

from **PC1a** but then considerably decreases upon going to **PRD1a** in the reaction of **1**. And, (4) the electron population of the $NSiMe_3$ moiety moderately decreases upon going to **TS1a** from the reactant but considerably increases upon going to **PRD1a** from **TS1a**. The most important differences in population changes between the Ti and Pt(0) complexes are found in the electron populations of the Ti, H, and CH_3 groups. The increase in the Ti atomic population at **PC1a** is attributed to the CT from methane to the Ti center; remember that the $C^{\alpha}-H$ bond of methane interacts with the Ti center in **1** like an agostic interaction, which involves the CT from the C−H bonding orbital to the Ti center.[37−39] In **TS1a**, the CH_3 electron population considerably increases but the H atomic population considerably decreases, while both electron populations of the H and CH_3 groups increase in **TS2**. These differences indicate that the C−H σ-bond activation by the Ti complex can be understood in terms of heterolytic C−H σ-bond activation unlike the oxidative addition by **2**. Also, it is noted that the Ti atomic population increases in **TS1a**, but the Pt atomic population decreases in **TS2**. These results suggest that the CT from methane to the Ti center participates in **TS1a** but the CT from the Pt center to methane participates in **TS2**, which will be discussed below in more detail.

Although important orbital interaction was well understood in the oxidative addition reaction,[2,7f,42] the orbital interaction has not been discussed yet in the heterolytic C−H σ-bond activation. Thus, it is worth investigating what type of orbital interaction is important in the heterolytic C−H σ-bond activation. As shown in Figure 3, the 83-rd MO in **PC1a** becomes stable in energy upon going from **PC1a** to **PRD1a**. This MO mainly consists of the sp^3 orbital of the CH_3 group and the $d_\pi-p_\pi$ orbital of the Ti−N moiety, as shown in Figure 4A. To inspect the orbital picture, we analyzed this MO by representing it with a linear combination of molecular orbitals of fragments[43]

$$\psi_i(\mathrm{AB}) = \sum_m C_{im}^{\mathrm{A}}\,\varphi_m(\mathrm{A}) + \sum_n C_{in}^{\mathrm{B}}\,\varphi_n(\mathrm{B}) \qquad (1)$$

where ψ_i(AB) represents the *i*-th MO of the system AB, φ_m(A) is the *m*-th MO of the fragment A, and C_{im}^{A} is the expansion coefficient of φ_m(A). Here, we separate the reaction system into methane and the Ti-imido complex. The weights of fragment orbitals are summarized in Table 2;[44] see Figure 4 for the important MOs of the reaction system and fragments. In the reaction by **1**, the 83-rd MO of the reaction system largely involves the $d_\pi-p_\pi$ bonding orbital of the Ti-imido moiety and somewhat the HOMO and LUMO of methane. Also, the d_{z^2} orbital of Ti, which is an unoccupied orbital in a formal sense, moderately participates in the 83-rd MO. These orbital mixings are schematically shown in Scheme 1; the $d_\pi-p_\pi$ bonding orbital suffers from antibonding overlap with the C−H σ-bonding orbital (HOMO) of methane, because the HOMO of methane is at lower energy than the $d_\pi-p_\pi$ bonding orbital. The C−H σ*-antibonding orbital (LUMO) of methane mixes with the $d_\pi-p_\pi$ bonding orbital in a bonding way, because the LUMO is at higher energy than the $d_\pi-p_\pi$ bonding orbital. These orbital mixings decrease the contribution of the H 1s orbital to the MO of the reaction system and increase that of the CH_3 sp^3 orbital. As a result, the CH_3 electron population increases and the H atomic population decreases; in other words, the H atom becomes proton-like and the CH_3 group becomes anionic. The empty d_{z^2} orbital overlaps with the CH_3 sp^3 orbital in a bonding way to form the CT interaction with the negatively charged CH_3 group, which increases the Ti atomic population. Also, the negatively charged CH_3 group forms an electrostatic stabilization interaction with the positively charged Ti center. Thus, the interactions shown in Scheme 1 clearly explain population changes by the heterolytic C−H σ-bond activation and Ti−CH_3 and C−H bond formations. In the reaction by **2**, the 32-nd MO of the reaction system is important. This mainly consists of the Pt d_π orbital and the LUMO of methane which is C−H σ*-antibonding orbital, as shown in Table 2; see Figure 4 and Figure S4 for these orbital pictures. It is noted that the HOMO of methane, which is a C−H σ-bonding orbital, participates little in this 32-nd MO. This means that only CT from $Pt(PH_3)_2$ to

Table 2. Weight of Fragment MOs Calculated with the B3LYP/BS2 Method

	$(Me_3SiO)_2Ti(=NSiMe_3)$		$Pt(PH_3)_2$[a]	
	82-nd MO	3.1%	28-th MO	0.0%
unocc	80-th MO	7.3%		
occ	78th-MO	56.8%	27-th MO	78.4%
			23-rd MO	1.0%
			22-nd MO	0.0%
	CH_4		CH_4	
	10-th MO	1.2%	10-th MO	0.8%
	7-th MO	2.0%	7-th MO	2.5%
unocc	6-th MO	10.4%	6-th MO	11.4%
occ	5-th MO	10.3%	5-th MO	0.6%
	3-rd MO	5.3%	3-rd MO	4.2%

[a] The analysis was made at the same C−H distance of methane as that of **TS1a**. The geometry is almost the same as that of **TS2**; see Supporting Information Figure S3.

Scheme 1

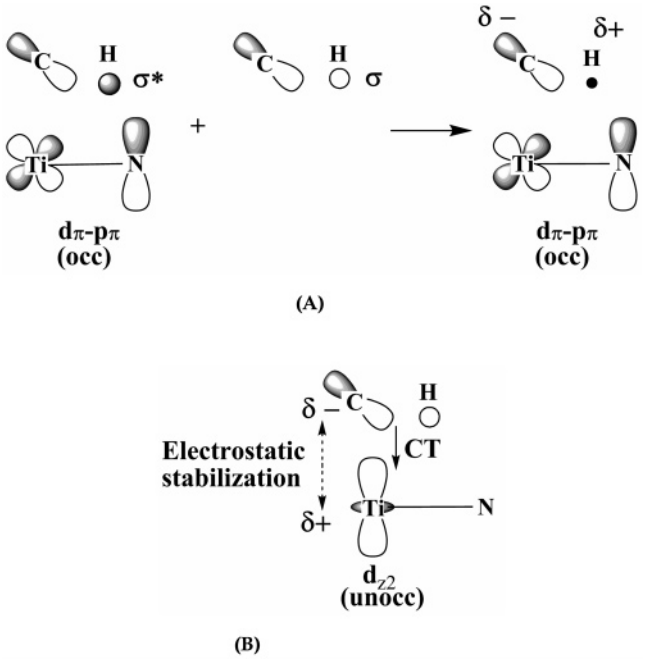

(42) (a) McKinney, R. J.; Thorn, D. L.; Hoffmann, R.; Stockis, A. *J. Am. Chem. Soc.* **1981**, *103*, 2595. (b) Tatsumi, K.; Hoffmann, R.; Yamamoto, A.; Stille, J. K. *Bull. Chem. Soc. Jpn.* **1981**, *54*, 1857.
(43) Similar methods were reported in several literatures: Kato, S.; Yamabe, S.; Fukui, K. *J. Chem. Phys.* **1974**, *60*, 572. Dapprich, S.; Frenking, G. *J. Phys. Chem.* **1995**, *99*, 9352.
(44) The weight was evaluated with a Mulliken approximation.

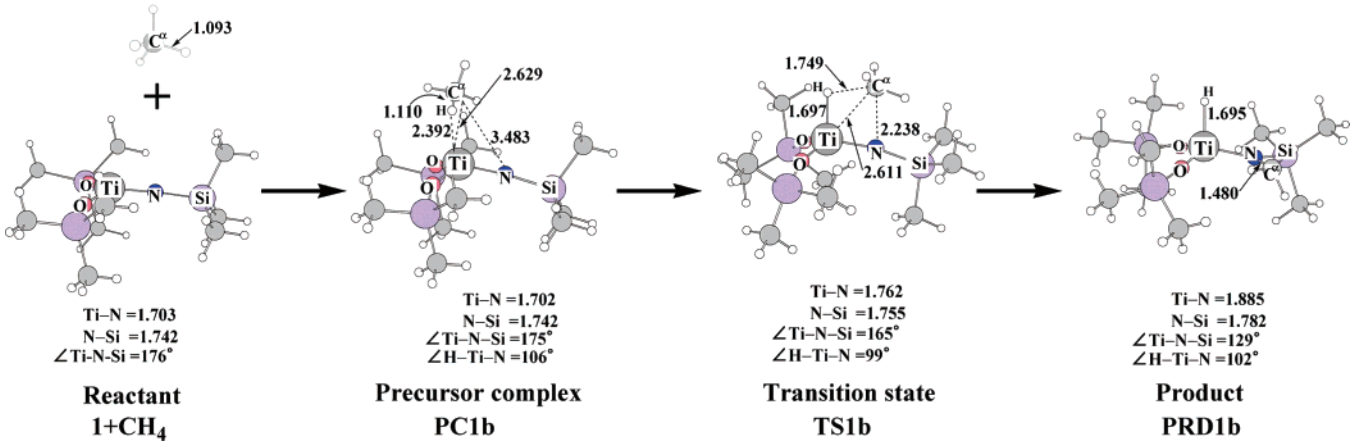

Figure 5. Geometry changes in the C−H σ-bond activation of methane by $(Me_3SiO)_2Ti(=NSiMe_3)$ **1** leading to formations of Ti−H and N−CH_3 bonds. Bond lengths are in angstroms, and bond angles are in degrees.

methane is important in the reaction by **2**, which is consistent with the population changes of this reaction (see Figure 2B); remember that the Pt atomic population decreases and both H and CH_3 electron populations increase in the reaction.

Because the occupied $d_\pi-p_\pi$ bonding orbital and the unoccupied d_{z^2} orbital play important roles in these orbital mixings around the transition state, the higher the occupied $d_\pi-p_\pi$ bonding orbital energy is and the lower the unoccupied d_{z^2} orbital energy is, the easier heterolytic C−H σ-bond activation becomes.

Upon going to **PRD1a** from **TS1a**, the Ti atomic population considerably decreases but the electron populations of $NSiMe_3$ considerably increase in the reaction by **1**. Those population charges are different from those observed upon going to **TS1a** from **PC1a**, indicating that the origin of those population changes are different from the above-discussed orbital interaction. One of the plausible reasons of these population changes is that the proton-like H atom binds with $NSiMe_3$ to suppress the electron donation from these ligands to the Ti center. As a result, the Ti atomic population considerably decreases and the electron population of the $NSiMe_3$ moiety considerably increases.

Effects of the OR Ligand on the C−H σ-Bond Activation: Here, we wish to mention ligand effects of the C−H σ-bond activation, because the O atom effect on the O−H σ-bond activation was discussed recently.[45] To clarify how much the OR ligand of **1** facilitates the C−H σ-bond activation, we compared the reactivity of $(HO)_2Ti(=NSiH_3)$ $\mathbf{1_{OH}}$ with that of $(HS)_2Ti(=NSiH_3)$ $\mathbf{1_{SH}}$, where $\mathbf{1_{OH}}$ is a good model of **1** because the C−H σ-bond activation reaction by $\mathbf{1_{OH}}$ occurs with similar BE, E_a, and ΔE values to those of the reaction by **1**; see Supporting Information Tables S3 and S4 and Figure S5 for energy, population, and geometry changes by the reactions of $\mathbf{1_{OH}}$ and $\mathbf{1_{SH}}$. Interestingly, the C−H σ-bond activation by $\mathbf{1_{SH}}$ takes place with a considerably larger E_a value (19.6 kcal/mol) and considerably smaller exothermicity ($\Delta E = -12.4$ kcal/mol) than those of the reaction by $\mathbf{1_{OH}}$ ($E_a = 15.5$ kcal/mol and $\Delta E = -21.9$ kcal/mol), where the DFT/BS2//DFT/BS1 method was employed. The $d_\pi-p_\pi$ and d_{z^2} orbitals of $\mathbf{1_{SH}}$ are at lower energy (−8.13 and −3.33 eV, respectively) than those of $\mathbf{1_{OH}}$ (−7.35 and −2.94 eV, respectively), where Kohn−Sham orbital energies are given. It is noted also that the Ti center is much more positively charged and the N atom is more negatively charged in $\mathbf{1_{OH}}$ than in $\mathbf{1_{SH}}$; the Ti and N atomic charges are +1.779e and −1.227e, respectively, in $\mathbf{1_{OH}}$ and +1.194e and −1.062e, respectively, in $\mathbf{1_{SH}}$, where the DFT/BS2-calculated charges are given. These results suggest that $\mathbf{1_{OH}}$ forms the stronger CT from the $d_\pi-p_\pi$ orbital to the C−H σ^*-antibonding orbital and the stronger electrostatic stabilizations between the negatively charged CH_3 group and the positively charged Ti atom and between the positively charged H and negatively charged N atoms than does $\mathbf{1_{SH}}$. Because of these factors, $\mathbf{1_{OH}}$ is more reactive than $\mathbf{1_{SH}}$; in other words, the OR group facilitates the heterolytic C−H σ-bond activation than the similar SR group.

Why does the H atom bind not with the Ti center but with the N atom? In the C−H σ-bond activation reaction by **1**, the methyl group is bound with the Ti center and the H atom is bound with the N atom.[36] It is of considerable interest to clarify the reason why the methyl group is not bound with the N atom but with the Ti center, and why the H atom is not bound with the Ti center but with the N atom.

We investigated the C−H σ-bond activation of methane leading to the formation of $(Me_3SiO)Ti(H)\{NMe(SiMe_3)\}$ **PRD1b**, which involves the Ti−H and N−CH_3 bonds. This is called the reverse regioselective reaction. In the precursor complex **PC1b**, methane approaches the Ti center in a different orientation from that in **PC1a**, as shown in Figure 5. In the transition state **TS1b**, the C^α−H distance of methane lengthens by 0.639 Å. This distance is longer than that of **TS1a**. The Ti−H distance in **TS1b** is almost the same as that of the product, **PRD1b**. These features indicate that **TS1b** is characterized to be more product-like than **TS1a**. **PRD1b** takes a pseudo-tetrahedral geometry similar to that of **PRD1a**.

As shown in Table 3, the BE value of **PC1b** is almost the same as that of **PC1a**. However, the E_a value for **TS1b** is much larger than that for **TS1a**. Consistent with the larger E_a value, the ΔE value of the reverse regioselective reaction is less negative than that of the normal one. These results indicate that the reverse regioselective reaction is thermodynamically and kinetically less favorable than the normal one. To understand the reasons why the normal regioselective reaction more favorably occurs than the reverse one, we evaluated here the Ti−H, Ti−CH_3, N−CH_3, and N−H bond energies, considering following assumed reactions; the Ti−H and Ti−CH_3 bond

(45) Teo, S.-X.; Wnag, G.-C.; Bu, X.-H. *J. Phys. Chem. B* **2006**, *110*, 26045.

Table 3. Binding Energy (BE), Activation Barrier (E_a), and Reaction Energy (ΔE) of the Reverse Regioselective C−H σ-bond Activation of Methane by $(Me_3SiO)_2Ti(=NSiMe_3)$ **1** Leading to Formation of $(Me_3SiO)_2Ti(H)\{N(CH_3)(SiMe_3)\}$[a]

	$(Me_3SiO)_2Ti(=NSiMe_3) + CH_4$		
	BE[b]	E_a[c]	ΔE[d]
MP2	−9.8	70.7	3.1
MP3	−7.2	61.8	−15.5
MP4(DQ)	−7.9	69.3	−5.9
MP4(SDQ)	−9.5	75.5	1.4
DFT(B3LYP)	−4.2	60.4	−1.2

[a] In kcal/mol unit. [b] BE = E_t(precursor complex) − E_t(sum of reactants). [c] E_a = E_t(transition state) − E_t(precursor complex). [d] ΔE = E_t(product) − E_t(sum of reactants).

Table 4. Ti−H, Ti−CH_3, Ti−NH_3, N−H, and N−CH_3 Bond Energies[a]

	B3LYP	MP2	MP3	MP4(DQ)	MP4(SDQ)	CCSD(T)
			Imido Complex			
Ti−H	73.4	79.9	74.8	76.0	81.1	80.4
Ti−CH_3	77.2	92.4	81.8	81.0	86.3	87.6
Ti−NH_2	100.6	119.1	102.0	102.7	110.4	111.0
N−H	114.8	116.0	112.9	113.0	113.0	113.2
N−CH_3	89.0	98.2	90.5	89.9	90.3	91.6

[a] The BS2 was used. In kcal/mol unit.

energies of the Ti-imido complex were calculated with eqs 2 to 5. The other bond energies were defined as energy changes by eqs 6 and 7.

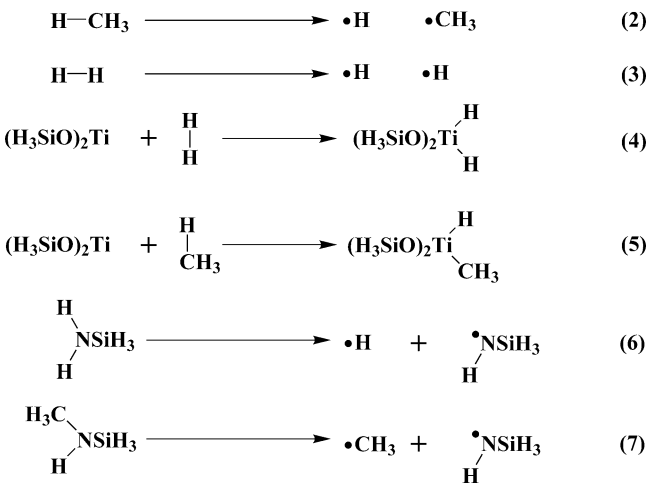

These bond energies are summarized in Table 4. The N−H bond energy depends little on the computational methods. The N−CH_3 bond energy moderately fluctuates upon going to the MP3 level from the MP2 level but converges upon going to the CCSD(T) level from the MP3 level. Moreover, the MP4-(SDQ)-, CCSD(T)-, and DFT-calculated N−CH_3 bond energies are similar to each other, suggesting that these methods present reliable N−CH_3 bond energies. Though the Ti−H and Ti−CH_3 bond energies moderately fluctuate around the MP2 level, they converge upon going to the MP4(SDQ) and CCSD(T) levels from the MP3 level. Also, the CCSD(T)-calculated Ti−H and Ti−CH_3 bond energies are similar to the MP4(SDQ)-calculated values, indicating that these values are reliable. Though the DFT-calculated Ti−H, Ti−CH_3, and Ti−NH_2 bond energies are moderately smaller than the CCSD(T)- and MP4(SDQ)-calculated values, the relative values of these bond energies are similarly calculated by the DFT, MP4(SDQ), and CCSD(T) methods.[41] Thus, the conclusion does not depend on the computational method.

Scheme 2

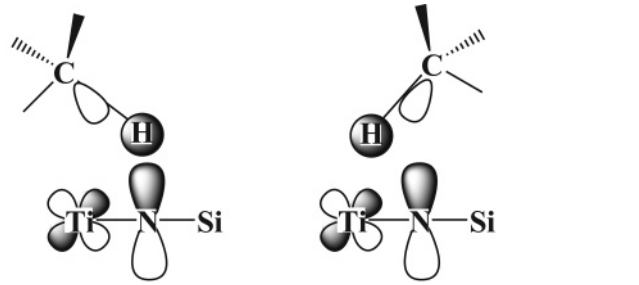

Apparently, the N−H bond is considerably stronger than the N−CH_3 bond, while the Ti−CH_3 bond is moderately stronger than the Ti−H bond. As a result, the normal regioselective reaction is more favorable than the reverse regioselective one from the thermodynamic point of view.

The higher E_a value of the reverse regioselective reaction is easily interpreted in terms of the smaller overlap of the C−H σ*-antibonding orbital with the $d_\pi-p_\pi$ bonding orbital of the Ti-imido moiety than that in the normal regioselective reaction. Methane approaches the Ti−N moiety with the H atom in the lead, as shown in Figure 1, because the H atom is less bulky than the CH_3 group. This approach leads to formation of a larger overlap between the H 1s orbital and the Ti−N $d_\pi-p_\pi$ orbital in the normal regioselective reaction than that in the reverse one, as shown in Scheme 2A, because the p orbital of the imido group contributes more to the $d_\pi-p_\pi$ orbital than the d_π orbital of Ti (Figure 4). In the reverse regioselective reaction, on the other hand, the H 1s orbital must interact with the d_π orbital of Ti. The methyl sp^3 orbital interacts with the imido p orbital, but it is much more distant from the imido group in the reverse regioselective reaction than the H atom is in the normal one (see Figures 5). As a result, the overlap is much small in the reverse regioselective reaction, as shown in Scheme 2B. Because of the smaller overlap, the reverse regioselective reaction needs a larger E_a value, and therefore, the reverse regioselective reaction is less favorable kinetically than the normal one.[46]

N−H σ-Bond Activation of Ammonia. It is of considerable interest to investigate whether or not the N−H σ-bond activation of ammonia can be achieved by a Ti-imido complex, because this σ-bond activation is believed to be very difficult and only one successful result was recently reported with (PCP)(η^2-propene)Ir.[19] We investigated here the N−H σ-bond activation of ammonia by **1**. The Ti−N^α distance is 2.199 Å in **PC1c**, as shown in Figure 6, where N^α represents the N atom of ammonia and N represents that of the imido ligand, hereafter. The short Ti−N^α distance indicates that the typical coordinate bond is formed between Ti and NH_3, in contrast with the weak interaction between the Ti moiety and methane. Starting from **PC1c** the N−H σ-bond activation takes place through transition state **TS1c**, to afford the product **PRD1c**. In **TS1c**, the N^α−H

(46) The heterolytic C−H σ-bond cleavage of methane leading to $H^+ + CH_3^-$ gives rise to the destabilization energy of 442.3 kcal/mol but that leading to $H^- + CH_3^+$ gives the destabilization energy of 364.3 kcal/mol, where the DFT/BS2//DFT/BS1 method was employed; see Supporting Information Table S6 for the destabilization energies calculated with various methods. This trend is reverse to the normal regioselectivity, indicating that the interaction with the Ti center in the transition state and the bond energies are important factors for the regioselectivity.

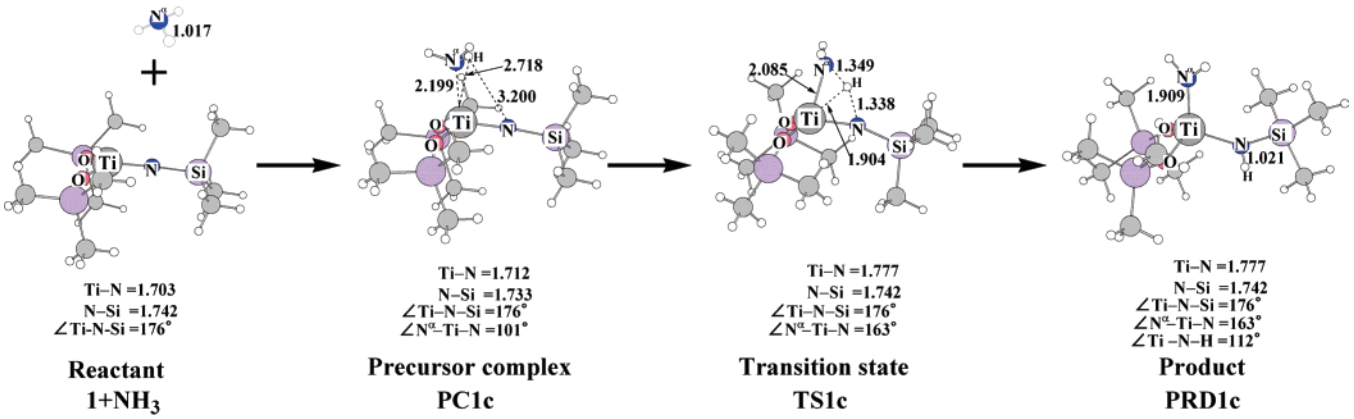

Figure 6. Geometry changes in the N—H σ-bond activation of ammonia by $(Me_3SiO)_2Ti(=NSiMe_3)$ **1**. Bond lengths are in angstroms, and bond angles are in degrees.

Table 5. Binding Energy (BE), Activation Barrier (E_a), and Reaction Energy (ΔE) of the N—H σ-Bond Activation of Ammonia by $(Me_3SiO)_2Ti(=NSiMe_3)$ **1** and $(PNP)Ti(\equiv CSiMe_3)$ **3**[a]

	$(Me_3SiO)_2Ti(=NSiMe_3)$ + NH_3			$(PNP)Ti(\equiv CSiMe_3)$ + NH_3		
	BE[a]	E_a[b]	ΔE[c]	BE[a]	E_a[b]	ΔE[c]
MP2	−36.0	25.0	−39.1	−30.7	13.3	−52.5
MP3	−37.1	18.9	−56.6	−29.8	5.8	−74.1
MP4(DQ)	−35.8	24.7	−46.4	−29.8	13.7	−57.8
MP4(SDQ)	−35.7	27.9	−39.4	−31.2	15.4	−56.3
DFT(B3LYP)	−31.4	19.0	−45.0	−24.8	7.5	−60.2

[a] In kcal/mol unit. [b] BE = E_t(precursor complex) − E_t(sum of reactants). [c] E_a = E_t(transition state) − E_t(precursor complex). [d] ΔE = E_t(product) − E_t(sum of reactants).

distance lengthens to 1.349 Å, which is considerably longer than that of free ammonia. The N—H distance between the ammonia and imido groups in **TS1c** is still long (1.338 Å). The Ti—N^α distance of **TS1c** is moderately longer than that of **PRD1c** but moderately shorter than that of **PC1c**. In **PRD1c**, the NH_2 moiety is planar, indicating that the NH_2 moiety is considered to be an imido anion.

As shown in Table 5, the BE value is considerably larger than those of the C—H σ-bond activation of methane. This is because ammonia coordinates with the Ti center by the CT from the lone pair of ammonia to the empty d orbital of Ti. Actually, the electron population of ammonia decreases very much in **PC1c**, as shown in Figure 8. The E_a value somewhat fluctuates around the MP2 and MP3 levels but much less upon going to the MP4(SDQ) level from the MP3 level. The DFT method presents a considerably smaller E_a value. However, it is noted that all the computational methods present a moderately larger E_a value and much larger exothermicity than those of the C—H σ-bond activation. This result suggests that the N—H σ-bond activation can be acheived by the Ti-imido complex, in which the activation barrier is moderately larger than the C—H σ-bond activation.

To search another complex which can easily perform the N—H σ-bond activation, we investigated the N—H σ-bond activation by the Ti-alkylidyne complex $(PNP)Ti(\equiv CSiMe_3)$ **3**, because the C—H σ-bond activation of benzene by **3** was recently reported in the experimental field.[18] This N—H σ-bond activation takes place through precursor complex **PC3** and transition state **TS3**, to afford product complex **PRD3**, as shown in Figure 7. Because the geometry changes are similar to those of the N—H σ-bond activation by **1**, we wish to omit a detailed explanation but mention several important points. In **TS3**, the N^α—H distance (1.310 Å) is shorter and the C—H distance (1.556 Å) is longer than the corresponding N^α—H and N—H distances of **TS1c**, indicating that **TS3** is more reactant-like than **TS1c**. In **PRD3**, the Ti—H distance is 2.309 Å and the Ti—C—H angle is 99°. These geometrical features indicate that the α-agostic interaction is formed in **PRD3**, which is in contrast to the absence of the agostic interaction in **PRD1c**. This interesting difference is easily interpreted in term of the energy levels of N—H and C—H σ-bonding orbitals. The C—H σ-bonding orbital is at −10.7 eV but the N—H σ-bonding orbital is at −17.1 eV, where Kohn—Sham orbital energies are given. Because the agostic interaction is formed by the CT from the C—H σ-bonding orbital to the empty d orbital, the C—H σ-bond is more favorable for the agostic interaction than the N—H σ-bond.

Consistent with the more reactant-like TS, the E_a value of this reaction is much smaller than that of the N—H σ-bond activation by **1**. It is noted that the E_a value is much smaller than that of the C—H σ-bond activation by **1**, which actually occurs experimentally. Thus, we wish to propose that the N—H σ-bond activation of ammonia can be easily achieved by the Ti-imido and Ti-alkylidyne complex and that the latter complex is much more reactive than the former one.

In this N—H σ-bond activation, the N^α—H bond should be broken, and the Ti—$N^\alpha H_2$ bond and either N—H or C—H bond are formed. The N—H bond energy is slightly larger than the C—H bond energy, as shown in Table 5. Thus, the considerably large exothermicity of the N—H σ-bond activation arises from the formation of the very strong Ti—$N^\alpha H_2$ bond. Because of this very strong Ti—$N^\alpha H_2$ bond, the product is more stable than the reactant complex.

Population changes show somewhat different features from those of the C—H σ-bond activation, as shown in Figure 8. As mentioned above, the electron population of ammonia considerably deceases in the precursor complexes **PC1c** and **PC3**, indicating that the strong CT interaction is formed between the Ti center and ammonia. In the transition state, the electron population of the NH_2 moiety considerably increases. The H atomic population further decreases in the reaction by **1** but slightly increases in the reaction by **3**, while its atomic charge is still positive; the H atomic population is 0.449e and 0.389e in the reactions by **1** and **3**, respectively. These features indicate that the NH_2 moiety is becoming anion-like and the H atom is

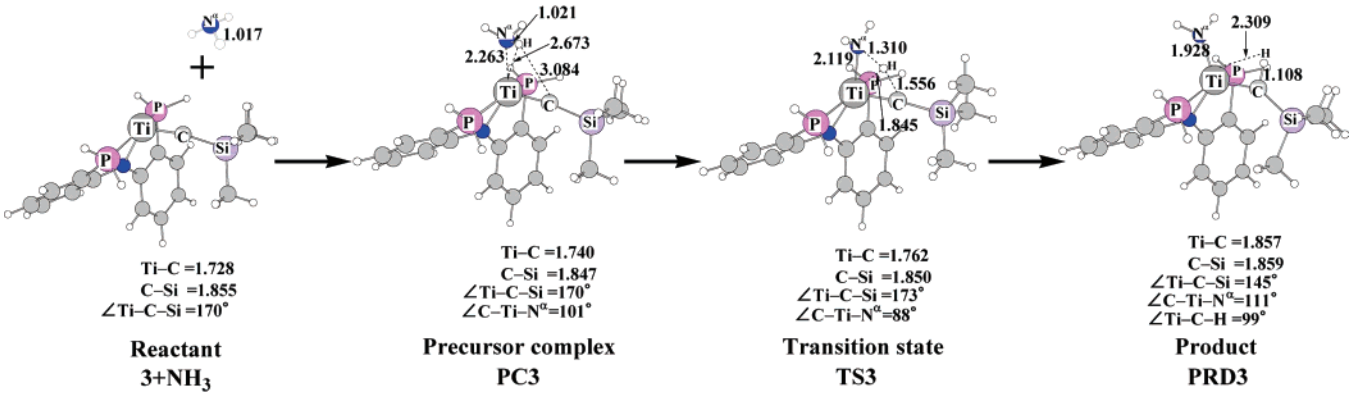

Figure 7. Geometry changes in the N—H σ-bond activation of ammonia by (PNP)Ti(≡CSiMe$_3$) **3**. Bond lengths are in angstroms, and bond angles are in degrees.

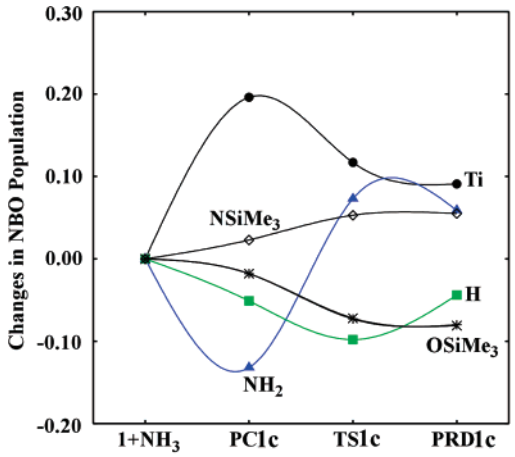

(A) $(Me_3SiO)_2Ti(=NSiMe_3)$ **1**

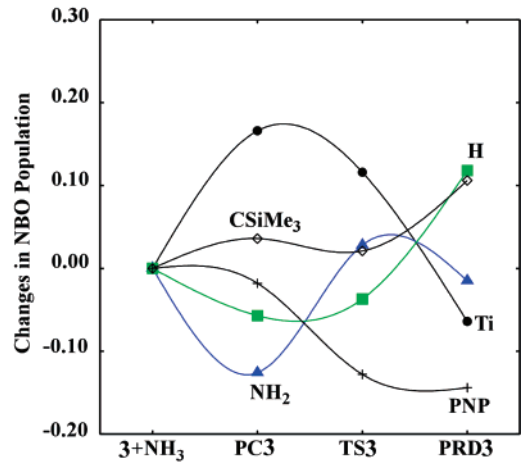

(B) (PNP)Ti(≡CSiMe$_3$) **3**

Figure 8. Population changes in N—H σ-bond activation of ammonia by (A) $(Me_3SiO)_2Ti(=NSiMe_3)$ **1** and (B) (PNP)Ti(≡CSiMe$_3$) **3**. The positive values represent the increase in electron population, and vice versa. The B3LYP/BS2 method was employed.

becoming proton-like in the transition state; in other words, the N—H σ-bond activation occurs in a heterolytic manner like the C—H σ-bond activation. Upon going to **PRD1c** and **PRD3** from **TS1c** and **TS3**, respectively, the Ti atomic population decreases. The reason is the same as that discussed in the C—H σ-bond activation of methane by **1**. The H atomic population is recovered in the reaction by **1**, because the H atom is again bound with the N atom. On the other hand, it considerably increases in the reaction by **3**, because it is bound with the C atom which is less electronegative than the N atom.

Conclusions

The C—H σ-bond activation of methane and the N—H σ-bond activation of ammonia by $(Me_3SiO)_2Ti(=NSiMe_3)$ **1** was theoretically investigated with the DFT, MP2 to MP4(SDQ), and CCSD(T) methods. The C—H σ-bond activation of methane proceeds through the precursor complex and the transition state, to afford the product $(Me_3SiO)_2Ti(Me)(NHSiMe_3)$. The activation barrier (E_a) is 14.6 (21.5) kcal/mol and the reaction energy (ΔE) is −22.7 (−16.5) kcal/mol, where the DFT- and MP4(SDQ)-calculated values are given without and in parentheses, respectively.

The analysis of the electron redistribution of this reaction shows interesting features, as follows: (1) The electron population of the CH_3 group considerably increases in the reaction, while the population of the H atom that reacts with the Ti-imido moiety considerably decreases in the transition state. These population changes indicate that the C—H σ-bond activation can be understood in terms of heterolytic C—H σ-bond activation unlike the oxidative addition. (2) The Ti atomic population considerably increases upon going to the transition state from the precursor complex, which indicates the CT from methane to the Ti center becomes stronger in the transition state. These characteristic features arise from orbital interactions among the $d_\pi-p_\pi$ bonding and d_{z^2} nonbonding orbitals of the Ti-imido moiety and the C—H σ-bonding and σ*-antibonding orbitals of methane. The CT interaction is formed between the $d_\pi-p_\pi$ bonding orbital and the C—H σ*-antibonding orbital, into which the C—H σ-bonding orbital mixes in an antibonding way with the $d_\pi-p_\pi$ bonding orbital. This orbital mixing decreases the H atomic population and increases the CH_3 electron population; in other words, the C—H bond to be broken is polarized by this orbital mixing. The negatively charged CH_3 group interacts with the empty d_{z^2} orbital of the Ti center, to form the CT interaction. Also, it forms an electrostatic interaction with the positively charged Ti center to yield the electrostatic stabilization. These population changes and interactions are completely different from those of the oxidative addition of methane to $Pt(PH_3)_2$. We wish to mention that the OR ligand is more favorable for the heterolytic C—H σ-bond activation than the SR ligand because of the stronger CT from the Ti-imido moiety to the C—H σ*-antibonding orbital and the

stronger electrostatic interactions between the negatively charged CH_3 group and the positively charged Ti center and between the positively charged H and negatively charged N atoms.

The reverse regioselective C−H σ-bond activation leading to $(Me_3SiO)_2Ti(H)\{NMe(SiMe_3)\}$ takes place with a larger E_a value and smaller exothermicity than the normal one. These results are interpreted in terms of bond energy and orbital overlap in the transition state. The Ti−CH_3 and N−H bonds are stronger than the Ti−H and N−CH_3 bonds, respectively, indicating that the normal regioselective C−H σ-bond activation is thermodynamically more favorable than the reverse one. Also, the H 1s orbital overlaps better with the $d_\pi-p_\pi$ bonding orbital of the Ti-imido moiety in the normal regioselective reaction than in the reverse one, indicating that the E_a value of the normal regioselective reaction is smaller than that of the reverse one.

The N−H σ-bond activations of ammonia by **1** and (PNP)-Ti(≡$CSiMe_3$) **3** (PNP = N-[2-$(PH_3)_2$-phenyl]) take place with a moderate activation barrier and a considerably large exothermicity. Several important results are summarized, as follows: (1) The BE value is considerably large, −31.4 (−35.7) and −24.8 (−31.2) kcal/mol for **1** and **3**, respectively. (2) Consistent with the large BE value, the electron population of the ammonia considerably decreases in precursors, **PC1c** and **PC3**, which indicates that the strong CT interaction is formed between the Ti center and NH_3. (3) The E_a and ΔE values are 19.0 (27.9) and −45.0 (−39.4) kcal/mol, respectively, in the reaction by **1** and 7.5 (15.4) and −60.2 (−56.3) kcal/mol, respectively, in the reaction by **3**. And, (4) the N−H σ-bond activation of ammonia occurs in a heterolytic manner like the C−H σ-bond activation of methane. From these computational results, we wish to propose that the N−H σ-bond activation can be achieved by Ti-imido and Ti-alkylidyne complexes.

In summary, we presented here a clear picture of orbital interaction in the heterolytic C−H σ-bond activation and theoretical proposals that Ti-imido and Ti-alkylidyne complexes can be applied to many heterolytic σ-bond activation reactions including N−H σ-bond activation.

Acknowledgment. This work was financially supported by Grant-in-Aids on basic research (No. 15350012), Priority Areas for "Molecular Theory for Real Systems" (No.461), Creative Scientific Research, NAREGI project from the Ministry of Education, Science, Sports, and Culture. Some of the theoretical calculations were performed with SGI Altix4700 workstations at the Institute for Molecular Science (Okazaki, Japan), and some of them were carried out with PC cluster computers at our laboratory.

Supporting Information Available: The full representation of ref 32. Structure of model complex $(OH)_2(THF)Ti(=NSiH_3)$ **1THF**(THF = tetrahydrofuran) (Figure S1). Optimized structure **1THF** with several basis sets and functionals (Table S1 and S2). Geometry changes in the C−H σ-bond activation of Ti-imido model complex $(H_3SiO)_2Ti(=NSiH_3)$, and $Pt(PH_3)_2$ complex (Figure S2 and S3). Molecular orbitals of $Pt(PH_3)_2$ of which geometry was taken to be the same as that of the transition state (Figure S4). Cartesian coordinates of all species. This material is available free of charge via the Internet at http://pubs.acs.org.

JA071825C